Int. J. Electrochem. Sci., 2 (**2007**) 29 - 51

International Journal of ELECTROCHEMICAL SCIENCE
www.electrochemsci.org

Electrochemical Measurements of Isopolyoxomolybdates: 1. pH Dependent Behavior of Sodium Molybdate

C. V. Krishnan[1,2], M. Garnett[1], B. Hsiao[2], and B. Chu[2]*

[1]Garnett McKeen Lab, Inc., 7 Shirley Street, Bohemia, NY 11716-1735, USA
[2]Department of Chemistry, Stony Brook University, Stony Brook, NY11794-3400, USA
[*]E-mail: ckrishnan@notes.cc.sunysb.edu ; tel. +6315890770; fax +6315890778

Received: 11 October 2006 / *Accepted:* 22 November 2006 / *Published:* 1 Januaray 2007

MoO_4^{2-} condenses on increasing acidity in aqueous solution and the extent of condensation depends on the level of pH. Frequency response analysis in the range 1000 Hz to 35 mHz and cyclic voltammetry were used to characterize the admittance, impedance, double layer capacitance, and semiconduction behavior of different protonated mono-, hepta- and octa- isopolyoxomolybdate species in solution. It was found that the dominant species was MoO_4^{2-} in the pH range 7-12 and the protonated species were of $Mo_7O_{24}^{6-}$ and of $Mo_8O_{26}^{4-}$ in the pH range 3-5 and below pH 2 respectively. This observation is consistent with the potentiometric titration data. Frequency as well as potential dependent color oscillations between blue and brown or gold at the mercury electrode were also observed. The results promise a new way of investigating polyoxometalates in solution.

Keywords: isopolyoxomolybdates, admittance, semiconduction, color oscillation

1. INTRODUCTION

A glimpse of the diversity and richness of polyoxometalate chemistry is obtained from recent reviews and books [1-8]. The oligomeric aggregates of the d^0 species of Mo(VI) were formed by the bridging of molecules. The first serious attempt to characterize the different oxomolybdate species at different acidities was based on potentiometric titrations [9,10]. The general conclusion from all the studies was that in alkaline solutions the molybdate species existed only as MoO_4^{2-}. At low molybdenum concentrations, the existence of significant amounts of $HMoO_4^-$ and H_2MoO_4 has also been postulated [10,11] before the hepta-molybdates are formed. In the literature one can often see different and often confusing ways of writing the formula for the same species. For example, H_2MoO_4 has been written as $Mo(OH)_6$ or $MoO_2(H_2O)_2(OH)_2$ or $MoO_3(H_2O)_3$ [12] and $HMoO_4^-$ has been written as $MoO_3(OH)^-$.

The convention used to indicate the number of protons involved in the formation of the appropriate species is as follows. 7 MoO_4^{2-} + 8 H^+ → $Mo_7O_{24}^{6-}$ + 4 H_2O so that the hepta-molybdate is indicated as $Mo_7O_{24}^{6-}$ (8, 7). Similarly the octa-molybdate $Mo_8O_{26}^{4-}$ is written as $Mo_8O_{26}^{4-}$(12, 8) because of the reaction 8 MoO_4^{2-} + 12 H^+ → $Mo_8O_{26}^{4-}$ + 6 H_2O. Thus, we follow the convention with MoO_4^{2-}(0, 1), $HMoO_4^-$(1, 1), and $H_2MoO_4^{2-}$(2, 1) for the monomers.

Ultracentrifugation studies [13] suggested an increase in polymerization when the number of protons bound per molybdenum, z, was changed from 0 to 1 with an average degree of polymerization of 6-9 when z = 1 – 1.5. Species with higher molecular masses were observed when z was > 1.5. These along with Raman spectral studies suggested hepta-molybdates at z = 1.14 and octa-molybdates at z ≈ 1.5. Counter ion binding studies with Na^+ and Li^+ were inconclusive. At very high acidities, cations, such as MoO_2^{2+}, were formed [14].

There are at least 3 forms of octa-molybdates, α-, β-, and γ-type, where the γ-form is an intermediate in the $\alpha \Leftrightarrow \beta$ inter-conversion. The α or β form of $Mo_8O_{26}^{4-}$(12, 8) could be crystallized from solutions of sodium molybdate in the pH range 3 – 4 by addition of organic cations [15]. All the 3 forms of octa-molybdates with disparate structures and crystals, where intermediate α-γ and β-γ forms are formed, have also been isolated [16]. In the high acid region, the formation of the large complex (34,19), and of the small $HMo_2O_6^+$ (5, 2) have also been reported [9]. The largest isopolyoxomolybdate reported [17] was $Mo_{36}O_{112}^{8-}$(64,36) with z = 1.8.

Judging from potentiometric data, the mononuclear molybdate condensed to form the hepta-molybdate. Experimental data lacked evidence for other species with less than 7 molybdenum atoms. However spectrophotometric data in 0.1M and 1M NaCl have provided evidence [12] for the species $HMo_2O_7^-$ with a formation constant $\log \beta_{3,2}$ of 14.6.

In order to carry out "rational" synthesis of novel and larger polyoxometalates systematically, one has to know the chemical nature and properties of simpler starting materials. When there are multiple equilibria involved as in the case of hydrolysis, multiple techniques that could provide more information are necessary in order to properly characterize the materials. This is evident from our studies because we can analyze the data based on several different electrochemical techniques, such as cyclic voltammetry, admittance, Nyquist and Bode plots, differential capacitance, and semi conduction.

2. EXPERIMENTAL PART

Analytical grade $Na_2MoO_4.2H_2O$, 1.0 M HCl and 1.0 M NaOH were used to prepare the molybdate solutions of varying acidities. No other background electrolyte was used for the measurements.

An EG & G PARC Model 303A SMDE tri electrode system (mercury working electrode, platinum counter electrode and Ag/AgCl (saturated KCl, reference electrode) along with Autolab eco chemie was used for cyclic voltammetric and electrochemical impedance measurements at 298 K. The solutions, about 7 mL in a minicup, were purged with N_2 for about 10 minutes before each experiment. Impedance measurements were carried out in the frequency range 1000 Hz to 35 mHz. The amplitude of the sinusoidal perturbation signal was 10 mV.

3. RESULTS AND DISCUSSION

3.1 Cyclic Voltammetry

These measurements were made at a scan rate of 100 mV/s and the results for the third scan are shown in Figures 1 - 4. The measured pH did not correspond to the initial concentration of acid or base because of proton absorption by the molybdate species. We did not make any attempt to calculate, z, the number of moles of H^+ absorbed per mole of MoO_4^{2-} from the initial concentration of H^+ and the measured pH. Our main interest was in the electrochemical investigation of large molecular clusters of polyoxometalates. The sodium molybdate concentration used in the present studies corresponded to the

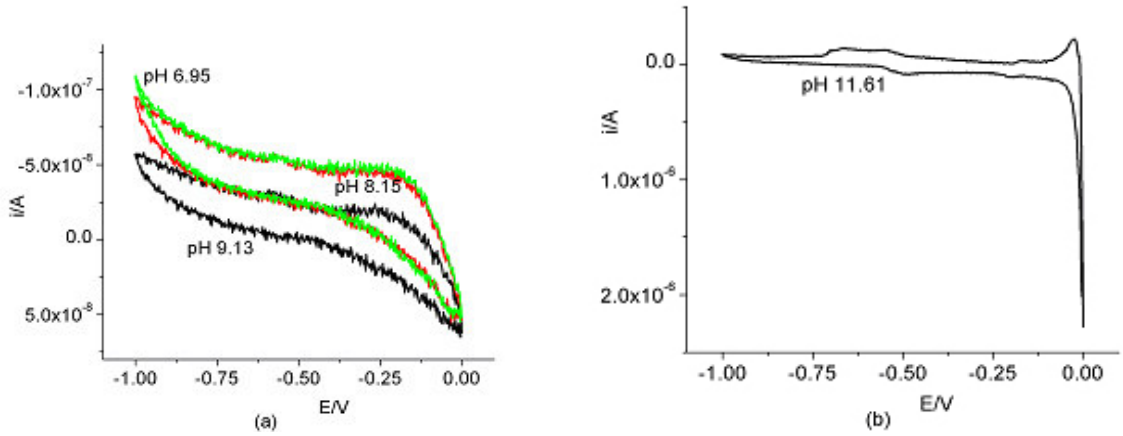

Figure 1. Cyclic voltammetry of 0.095 M sodium molybdate, pH = 7-12

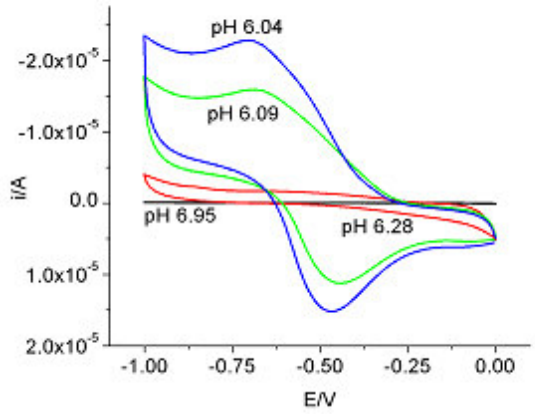

Figure 2. Cyclic voltammetry of 0.095 M sodium molybdate, pH = 6-7

molybdenum concentration used in the preparation of $(NH_4)_{42}[Mo_6^{VI}O_{21}(H_2O)_6]_{12}[Mo_2^{V}O_4(CH_3COO)]_{30}$·*ca.*300$H_2O$·*ca.*10 CH_3COONH_4 [18] so that it would be easier to compare the data for the complex with that of the simpler species. From the cyclic voltammograms, there were about 4 regions of similar behavior. In the pH range 7-12, as shown in Figure 1(a), there were no peaks and it corresponded to the non protonated MoO_4^{2-}(0, 1). At 11.61 pH, as shown in Figure 1(b), there was an anodic peak at -0.03V, indicating some passivation of mercury at

this potential and high pH value. The next region with change in the voltammetric peak was in the pH range 6-7, as shown in Figure 2. This region, that could be attributed to the formation of $HMoO_4^-$(1, 1) and H_2MoO_4(2, 1), corresponded to the same region in the potentiometric titrations data that were sensitive to the electrolyte and its concentration.

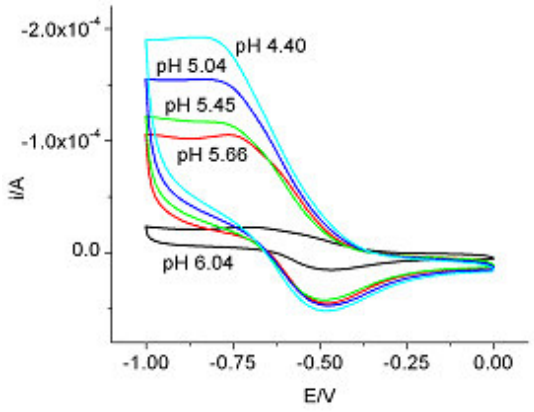

Figure 3. Cyclic voltammetry of 0.095 M sodium molybdate, pH = 4.4 - 6.0

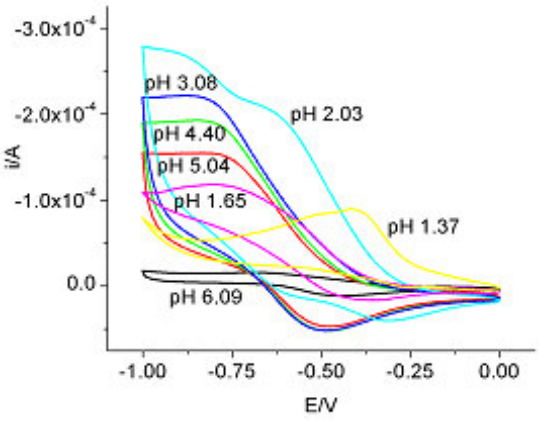

Figure 4. Cyclic voltammetry of 0.095 M sodium molybdate at different acidities

The potentiometric data analysis using assumed species and assumed equilibrium constants indicated that hydrolysis started at approximately 0.6 pH units earlier when the Na^+ concentration was changed from 0.6 to 3.0 M. Hydrolysis seemed to start when z = 8/7 = 1.14. The third region in our studies, as shown in Figure 3, was in the pH range 4-6 and corresponded to the formation of hepta-molybdate, $Mo_7O_{24}^{6-}$ (8, 7) and their protonated species, $HMo_7O_{24}^{5-}$(9, 7), $H_2Mo_7O_{24}^{4-}$(10,7), and $H_3Mo_7O_{24}^{3-}$(11, 7). There was a disagreement as to whether $H_3Mo_7O_{24}^{3-}$(11,7) or $Mo_8O_{26}^{4-}$(12, 8) was formed. Figure 4 is a summary of the pH dependence. It shows that the final change appeared below pH 3.0, corresponding to the formation of octa-molybdates, $Mo_8O_{26}^{4-}$(12, 8). The nature of this species in solution could be deduced from typical potentiometric titrations [4] at constant ionic strength, as shown in Figure 5. Here z was the average number of moles of H^+ bound per mole of MoO_4^{2-} in solution.

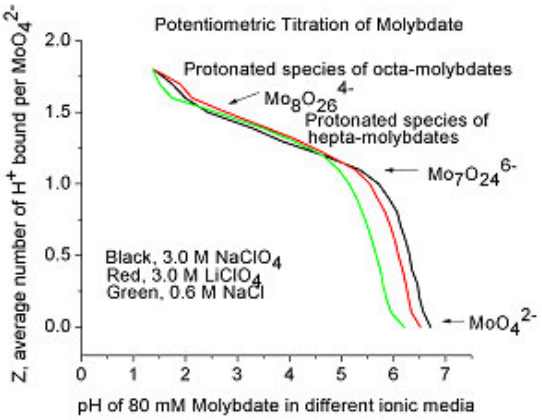

Figure 5. Potentiometric data for isopolyoxomolybdate species, adapted from [4], Page 140

The values of the overall (log)equilibrium constants derived from the data for β (1,1), β (2,1), (β8,7), β (9,7), β (10,7), and β (11,7) are 3.89, 7.50, 57.74, 62.14, 65.68, and 68.21, respectively [9]. From the shape and spacing of the potentiometric titration curves, Sasaki, Lindqvist and Sillen deduced that the first polynuclear complex formed was the hepta-molybdate [10]. Compared to potentiometric titration data, the cyclic voltammetric data provided clearer markings on the formation of different species by slight shifts in the cathodic and anodic peaks as well as differences in cathodic currents.

3.2 Frequency Response Analysis

3.2.1 Admittance

Admittance, Y, which is the inverse of impedance, is like a frequency dependent conductance. Like impedance, it has both real and imaginary parts. Since the overall admittance of parallel elements is the sum of individual admittances, admittance is a useful tool in the analysis of parallel circuits.

It has been observed [19-21] that admittance data can also provide information on the nature of solute –solvent interactions taking place at and near the electrode surface. We utilized this aspect of admittance to understand the nature of molybdate species at different acidities. Figure 6 shows the admittance of sodium molybdate at pH 11.61 at frequencies in the range 5 KHz to 100 Hz with potentials varying from 0 to – 1.0V. The data showed that the admittance increased initially when the frequency was decreased from 5 KHz to 1 KHz. With further decrease in frequency, the admittance became less. However the behavior at potentials – 0.25 to 0 V was significantly different for higher frequencies and lower frequencies. At frequencies such as 250 and 100 Hz and at much less negative potentials, there was an increasing trend in admittance and the value went through a maximum. This behavior is similar to the behavior of sodium or potassium chlorides in that the admittance increases at first with decreasing frequency and then decreases with further decrease in frequency. The behavior with change in potential was also similar to that of NaCl or KCl. The admittance behavior of sodium molybdate in the pH range 7 -11 was very similar. A typical example at 1000 Hz is shown in Figure 7. Judging from our experience with alkali halides [19], we concluded that the behavior exhibited in this pH range was mostly the behavior of the counter ion Na^+, but not that of MoO_4^{2-}. Changes in

orientation of water molecules at the electrode double layer could contribute to the observed admittance maxima near the potential zero.

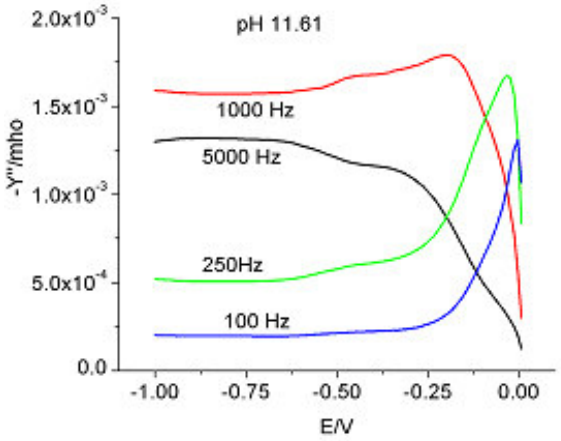

Figure 6. Admittance of 0.095 M sodium molybdate, pH 11.61

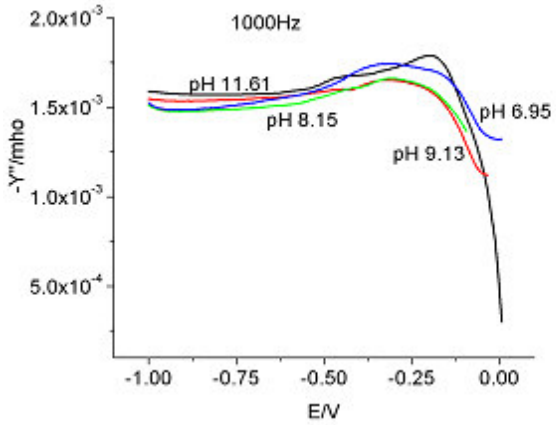

Figure 7. Admittance of 0.095 M sodium molybdate, pH 7-12

Figures 8 and 9 show the admittance data in the pH range 6 - 7 at 1000 Hz and 100 Hz respectively. The admittance decreased with decreasing pH, possibly due to the condensation of molybdate. However, the admittance behavior changed at less negative potentials. At pH 6.28, the admittance exhibited 2 peaks in the potential range 0 to – 0.25V at 1000 Hz. A broad shoulder at pH 6.95 was also indicative of the two peaks. But only one peak was observed at pH 6.09 and 6.04. Judging from the data at 100 Hz it appeared that the potential at which the peaks were exhibited was shifted to more negative potentials. There was a possibility that the protonated species of MoO_4^{2-} could be responsible for those peaks that were sensitive to frequency and potential. The kind of sensitivity shown here for admittance by different species of molybdates in solution could not be observed in other experimental

techniques used for the study of isopolyoxomolybdates. Of course, one could expect a substantial difference in interaction at and near the double layer when the species changed from MoO_4^{2-} to $HMoO_4^-$ to H_2MoO_4 before condensation. It is well known that solute-solvent interactions between large univalent ions or neutral molecules and water contribute to their thermodynamic properties [22, 23].

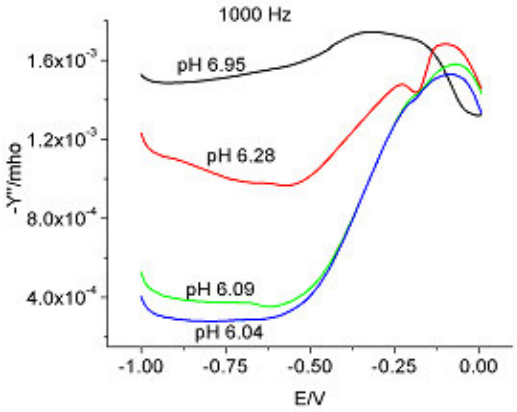

Figure 8. Admittance for 0.095 M sodium molybdate, pH 6-7, 1000 Hz

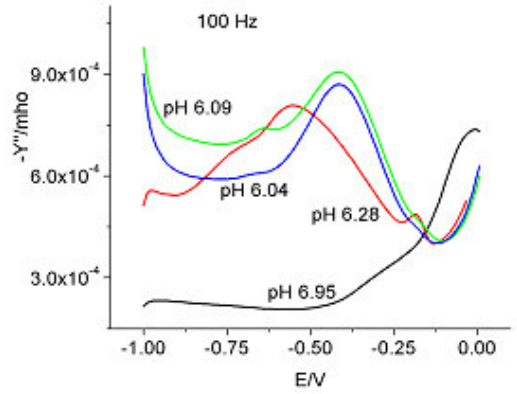

Figure 9. Admittance for 0.095 M sodium molybdate, pH = 6 – 7, 100 Hz

Figures 10 and 11 show the admittance data in the pH range 4 - 6 and at 1000 and 100 Hz, respectively. The admittance decreased with decreasing pH at both frequencies. While the admittance behavior at 1000 Hz was very similar, there was a pH-dependent shift in the peak of admittance at 100 Hz. Only one peak was observed at all the pH values with another shoulder for pH = 6.04 in the potential range of 0 to – 0.1V. Judging from the data at 100 Hz, as shown in Figure 11, the potential at which the peak was exhibited was shifted to more negative potentials. The continuous shift of this peak with decreasing pH strongly suggested the formation of the protonated species of $Mo_7O_{24}^{6-}$ and that these were sensitive to frequency and potential. Lower frequencies tended to discriminate better the different protonated species.

Judging from the sensitivity of the admittance data to frequency, water molecules could be playing a significant role in these polyoxomolybdates. It is known [24] that $MoO_3(OH)^-$ expands its coordination sphere by coordinating two water molecules to form $MoO(OH)_5^-$ as a prelude to condensation. The OH group trans to the Mo=O bond was weakly bound so that an oxo-bridge was formed by the reaction: $2[MoO(OH)_5]^- = [(HO)_4OMo\text{-}O\text{-}MoO(OH)_4]^{2-} + H_2O$.

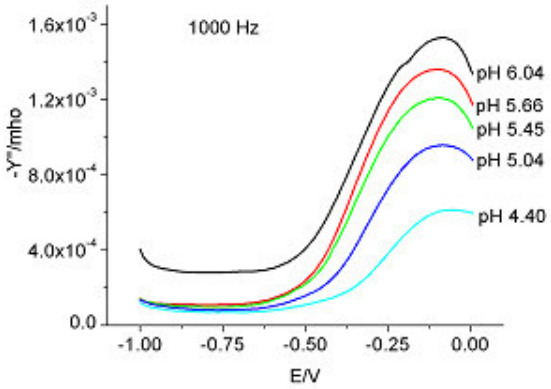

Figure 10. Admittance of 0.095 M sodium molybdate, pH 4 – 6, 1000 Hz

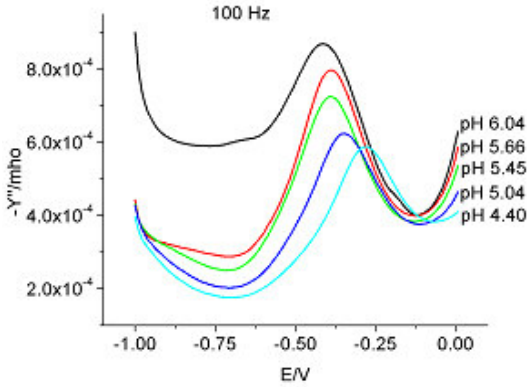

Figure 11. Admittance of 0.095 M sodium molybdate, pH 4 – 6, 100 Hz

Figure 12 shows the admittance data in the pH range 1.3 – 4.4 at 1000 Hz. We could not measure the complete admittance data at pH = 1.37 because the mercury drop was falling off during the measurement. The admittance increased at less negative potentials probably due to an increase in the concentration of the free acid. There was a dramatic change at pH values lower than 2, as exemplified by the data at pH 1.65. Figure 13 shows the data at 100 Hz. Judging from these data, the behavior at pH = 1.65 was completely different at 1000 Hz and 100 Hz. The data exhibited peaks where the shoulder peak corresponded to the species at pH values in the range 3-6. The second peak at more negative potentials suggested the formation of the octa-molybdate and its admittance behavior was different from that of the hepta-molybdate. The hepta- and octa-molybdates were also known [22] to exist in hydrated forms such as $[H_8Mo_7O_{28}]^{6-}$.

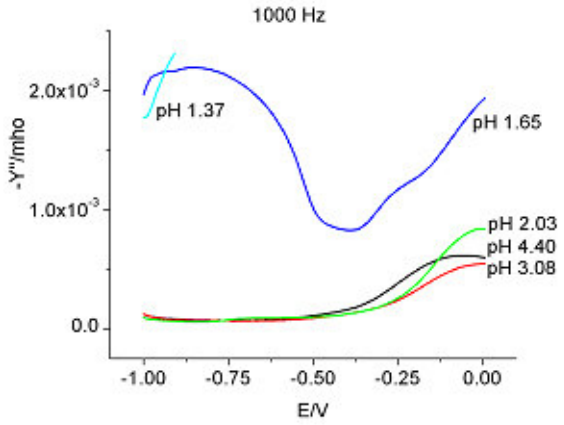

Figure 12. Admittance of 0.095 M sodium molybdate, pH 1.37- 4.40, 1000 Hz

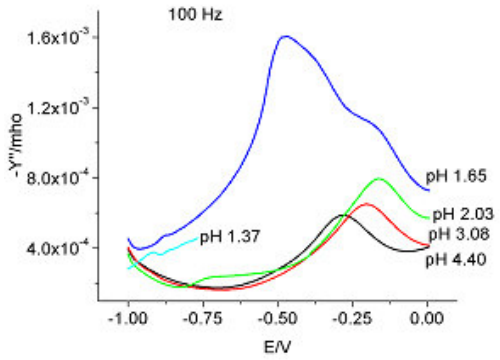

Figure 13. Admittance of 0.095 M sodium molybdate, pH 1.37- 4.40, 100 Hz

3.2.2 Nyquist and Bode Plots

The complex plane of Nyquist or Cole-Cole plots has frequency as the only implicit variable and allows us to determine the circuit elements. The Bode plots of $\log|Z|$ and phase angle Φ vs. $\log(\omega)$ is a better representation of the frequency variation of Z' and Z''. Each maximum in these graphs represents a separate relaxation process or time constant and may be associated with processes characterized by surface-state concentrations.

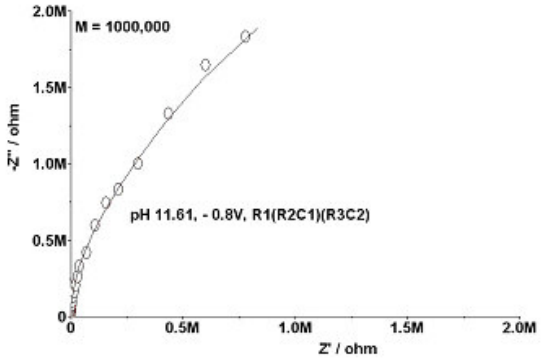

Figure 14. Sodium molybdate, 0.095 M, pH 11.61, – 0.8 V; Nyquist Plot

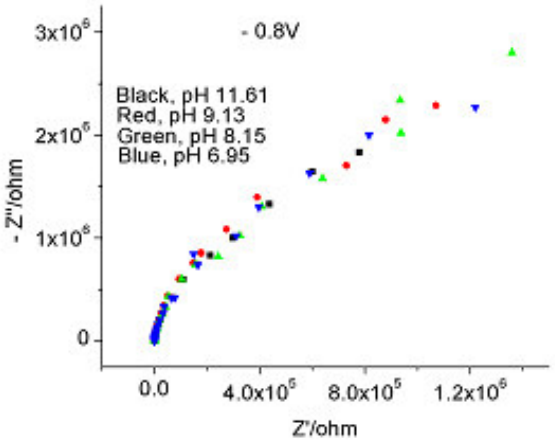

Figure 15. Sodium molybdate, 0.095 M, pH 7 –12, – 0.8 V; Nyquist Plot

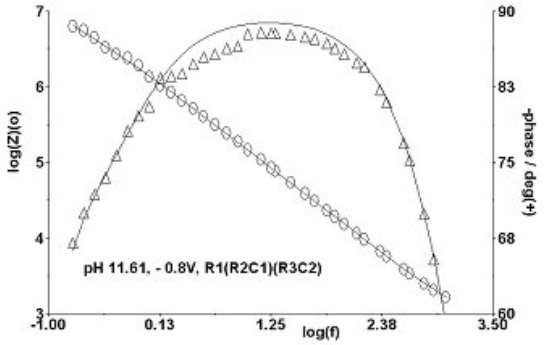

Figure 16. Sodium molybdate, 0.095 M, pH 11.61, – 0.8 V; Bode Plot

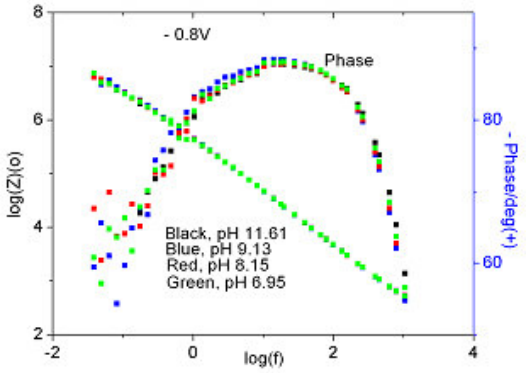

Figure 17. Sodium molybdate, 0.095 M, pH 7 –11, – 0.8 V; Bode Plot

Very similar Nyquist plots and Bode plots observed at pH 11.61, 9.13, 8.15, 8.12, and 6.95 and at -0.8V are shown in Figures 14-17. The intercept with the real axis at high frequencies could be attributed to the bulk resistance of the electrolyte whereas the intercept at low frequencies was a measure of the polarization resistance. This polarization resistance is the sum of all resistances due to film formation, electrolyte in the pores and charge transfer or corrosion reaction at the substrate/electrolyte interface. The data could be fitted with the equivalent circuit, R1(R2C1)(R3C2). Deviations from the normal phase angle behavior occurred at a frequency below 10 Hz. The fit was

better with R1(R2C1)(R3C2)(R4C3) at pH 6.95. We had observed a similar behavior at -0.6V. The data at -0.6V were almost super imposable with -0.8V data and they all fitted the equivalent circuit R1(R2C1)(R3C2). The observed phase angle was close to $\pi/2$ and was purely capacitive. These results definitely suggested that there was only one species in the pH range 7-12 and the species could be the simple $MoO4^{2-}$, because most of the contributions observed in these figures could be attributed to Na^{+} only.

The Nyquist and Bode plots at -0.8V and -0.6V in the pH range 4-6 are shown in Figures 18-21. For the sake of clarity, only the phase angle is shown in the Bode plots in Figures 20-21. The impedance became less and less with decreasing values in pH and the values were extremely small by a factor of about 100 when compared to the impedance values observed above pH 7. Thus, the behavior was becoming less capacitive with decreasing values in pH. Since the polarization resistance was less and less with decreasing pH, the adsorbed film should be very weak and became more and more defective or porous, permitting the electrolyte to penetrate through to the substrate. Also, the phase deviated from the purely capacitive value of $\pi/2$ and the deviation increased with decreasing pH. While the phase data at -0.8V showed only one relaxation process, the one at -0.6V showed two relaxation

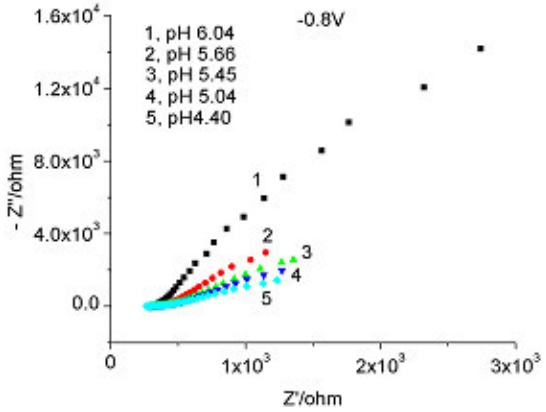

Figure 18. Nyquist plot for 0.095 M sodium molybdate, pH 4 – 6, – 0.8 V, 1000 Hz – 35 mHz.

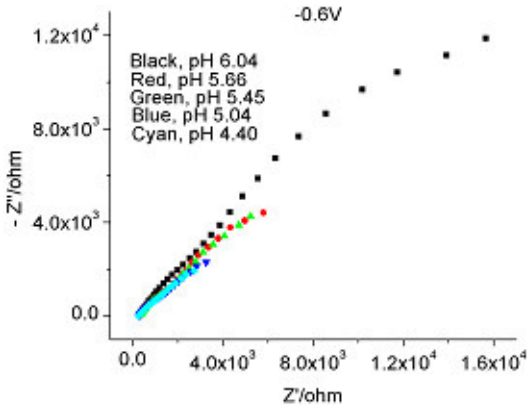

Figure 19. Nyquist plot for 0.095 M sodium molybdate, pH 4 – 6, – 0.6 V, 1000 Hz – 35 mHz

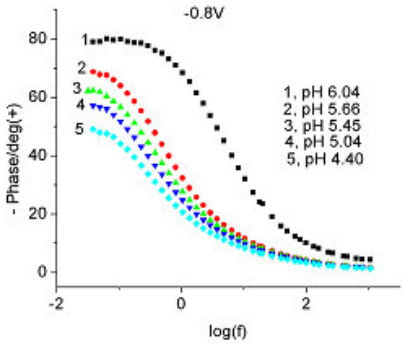

Figure 20. Bode plot (phase only) for 0.095 M sodium molybdate, pH 4 – 6, – 0.8 V, 1000 Hz –35 mHz.

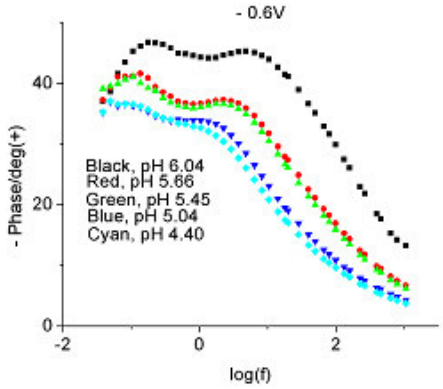

Figure 21. Bode plot (phase only) for 0.095 M sodium molybdate, pH 4 – 6, – 0.6 V, 1000 Hz – 35 mHz.

processes, especially at pH values closer to 6. The distinction between the two peaks became less and less as the pH value got lower and lower, due likely to the different species present in the solution at intermediate pH values and more and more hepta-molybdate being formed at the lower pH values. The high frequency relaxation process could normally be attributed to the adsorbed film/solution interface and represented the dielectric characteristics of the adsorbed film. On the other hand, the low frequency process was normally associated with the substrate/solution interface and represented the process of localized corrosion that took place in the substrate through the pores of the film.

The Nyquist and Bode plots at -0.8 V for the pH range 4.4 to 1.3 are shown in Figures 22-23. For the sake of clarity only the phase angle is shown in the Bode plots in Figure 23. The impedance values further decreased with a further decrease in the pH value from 4.4 to 1.3. This was also true with the decrease in phase angle. The impedance data at pH 1.65 and 1.37 are not included in Figure 22 because of their much higher values whereas the data are included in the Bode plot in Figure 23. It is obvious that there was a dramatic shift in the behavior below pH 2. This is probably due to the formation of octa-molybdates, instead of hepta-molybdates. A change in behavior was also noted in the cyclic

voltammetric peaks at pH = 2.03, 1.65 and 1.37, where both cathodic and anodic peaks shifted towards less negative values.

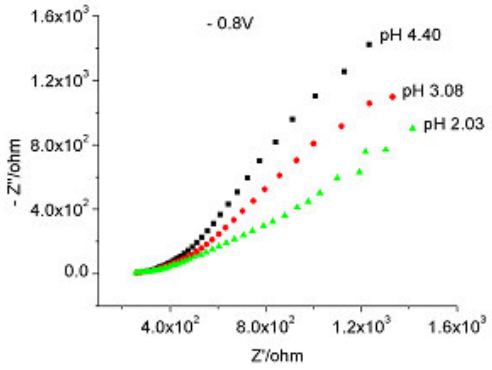

Figure 22. Nyquist plot for 0.095 M sodium molybdate below pH 4, – 0.8V, 1000 Hz – 35 mHz.

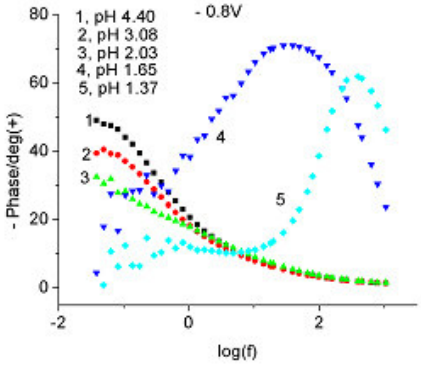

Figure 23. Bode plot (phase only) for 0.095 M sodium molybdate below pH 4.04 and at – 0.8 V, 1000 Hz – 35 mHz.

3.2.3 Differential Capacity:

Double layer capacitance, C_{dl}, is generally obtained from differential capacitance measurements when ohmic resistance is compensated. In such a case, C_{dl} should be independent of frequency.

The capacitance data at pH 11.61 and at different frequencies, as shown in Figure 24, are somewhat similar to that observed for NaCl. Very similar behavior was observed in the pH range 7-12 for these plots. However, Figure 24(a) for 5000 Hz, shown in an expanded window, indicated a small peak or hump at about -0.43V. This behavior was seen for other frequencies as well. At this point we could only speculate on the source of this hump. This may be due to the differing competition between the negative charge of the molybdate and the negative charge of the electrode for the positively charged sodium ion and the corresponding orientation changes of water around these ions.

The capacitance data in the pH range 4-6 at 1000 and 100 Hz are shown in Figures 25 and 26 respectively. These data showed the frequency dependence of capacitance. The capacitance increased with decreasing pH values and with decreasing frequency. There was only one capacitance peak at both frequencies except for the solution at pH 6.04 where two humps were observed. Even though we observed a shift in peak potentials for different pH at 100 Hz, such behavior was not observed here, indicating the insensitivity of the capacitance peaks to protonation of the species.

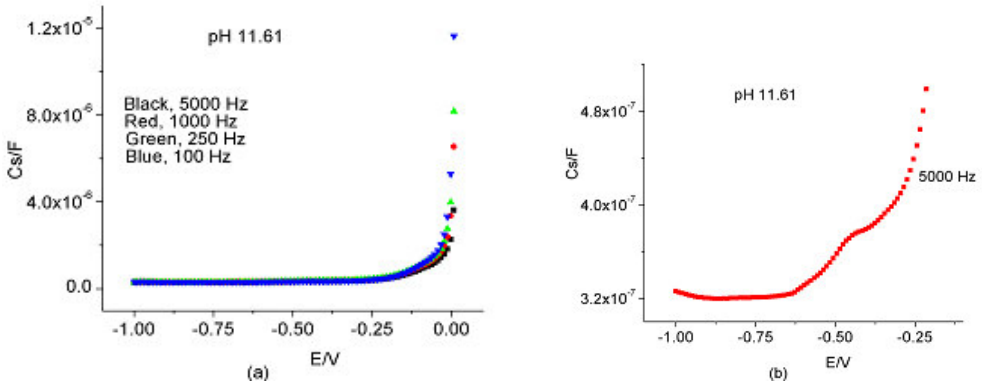

Figure 24. Differential capacitance of 0.095 M sodium molybdate, pH 11.61

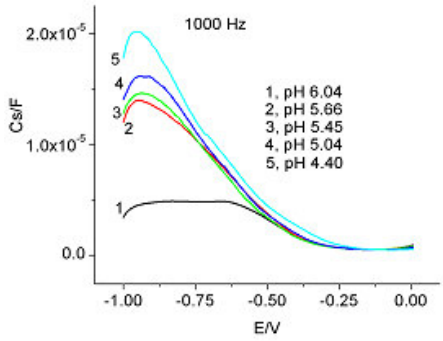

Figure 25. Differential capacitance of 0.095 M sodium molybdate, pH 4– 6, 1000 Hz

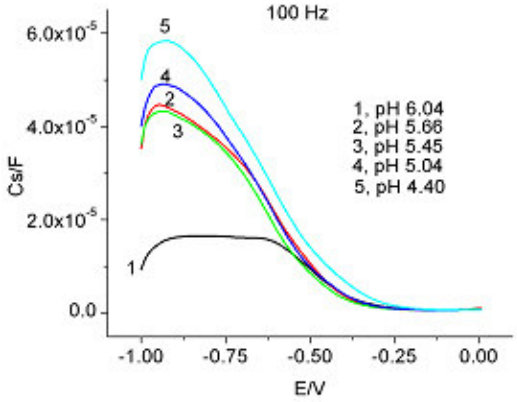

Figure 26. Differential capacitance of 0.095 M sodium molybdate, pH 4 – 6, 100 Hz

The capacitance data below pH 4 are shown in Figures 27 and 28. Here we also observed a capacitance dependence on frequency, with higher capacitance at lower frequency and the capacitance peak also shifted to much less negative potentials. Of course this was the region when octa-molybdates could be formed instead of the hepta-molybdates as indicated by the cyclic voltammetric data.

Frequency dependence of differential capacitance has also been observed for Ag(111) in 0.01 M NaCl [25] and has been attributed to the real surface with fractal characters instead of an ideal homogeneous electrode surface.

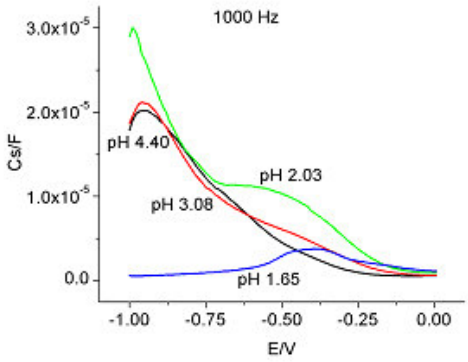

Figure 27. Differential capacitance of 0.095 M sodium molybdate below pH 4, 1000 Hz

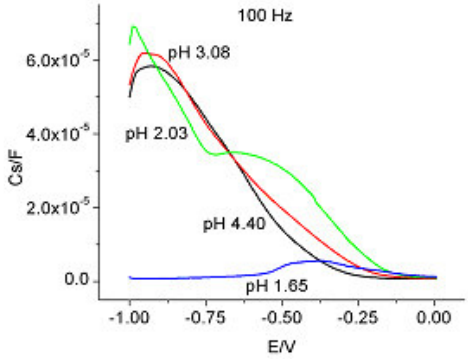

Figure 28. Differential capacitance of 0.095 M sodium molybdate below pH 4, 100 Hz

3.2.4 Semiconduction

Passive films on many metals and alloys exhibit semi-conductor behavior. An inner p-type oxide layer and an outer n-type hydroxide layer with a p-n hetero-junction have been suggested before [26, 27]. These passive films have characteristic capacitance that obeys the Mott-Schottky relationship. The Mott-Schottky equation that connects the space charge capacitance C of a p-type semiconductor and the electrode potential E is given as

$$C^{-2} = -[2/(q\varepsilon\ \varepsilon_0 N_A)]\ (E-E_{FB} + kT/q) \qquad (1)$$

where ε is the vacuum permittivity (8.85 x 10^{-14} F/cm), ε_0 the dielectric constant of the specimen, q the electron charge (1.602 x 10^{-19} Coulomb), k the Boltzmann constant (1.38 x 10^{-23} J/K), T the absolute temperature, N_A the acceptor density, and E_{FB} the flat band potential. At room temperature, kT/q is about 25 mV and can generally be neglected. The measured capacitance corresponds to the space charge capacitance provided that the Helmholtz capacitance and the surface state capacitance are negligible. The intercept on the potential axis gives the flat band potential. The slope of the C^{-2} versus E plot is inversely proportional to the doping concentration and can be obtained provided that the dielectric constant of the passive film is known. For passive films the donor or acceptor density generally corresponds to the non-stoichiometry of the passive films, instead of the impurity concentration, and is generally much higher than the values for ordinary bulk semiconductors [27]. Also for passive films formed on metals, the linear range of the Mott-Schottky plot is usually narrow compared to the normal semiconductors [27,28].

For many metals, the passivation is due to the formation of oxide films. The growth of the oxide film is due to the migration of both the cation and O^{2-} ion through the film under the influence of the high electric field of about a million volts per cm. The ionic current, i, responsible for the oxide growth is related to the field strength H by the expression: i = A exp(BH), where A and B are constants that depend on the electrolyte [26].

The Mott-Schottky plot, as shown in Figure 29 at pH 11.61 indicated a p-type semiconduction behavior similar to that of NaCl [19]. The same behavior was observed in the pH range 7-12. On the other hand, the Mott-Schottky plots, as shown in Figures 30 and 31, at 1000 and 100 Hz for the pH range 4.4 to 6 indicated an n-type behavior, due to the adsorbed species of molybdenum which had a valence state different from molybdenum(VI).

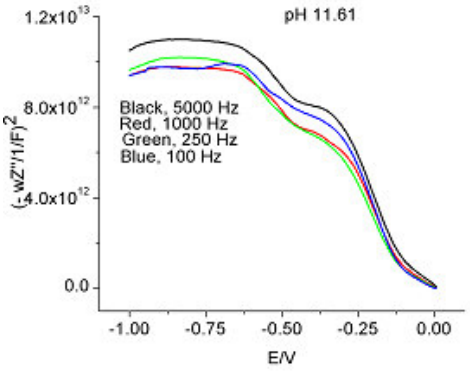

Figure 29. Mott-Schottky plot for 0.095 M sodium molybdate, pH 11.61

The Mott-Schottky plots shown in Figures 32 and 33 are for solutions at the highest acidities and at 1000 and 100 Hz respectively. The behavior below pH 2 was different from the pH range 2-6. The data at pH 1.65 exhibited both p-type and n-type semiconduction with different flat band potentials. We suggest that two reduced species, one from the hepta-molybdate and one from the octa-molybdate must be adsorbed at this pH contributing to two different behaviors with different flat band potentials. We could not get the data at pH 1.37 because the mercury drop was falling off. However the few data available seem to indicate the beginning of a p-type conduction behavior.

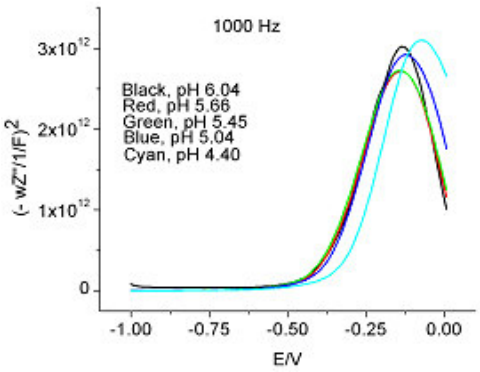

Figure 30. Mott-Schottky plot for 0.095 M sodium molybdate, pH 4.40 – 6.04, 1000 Hz

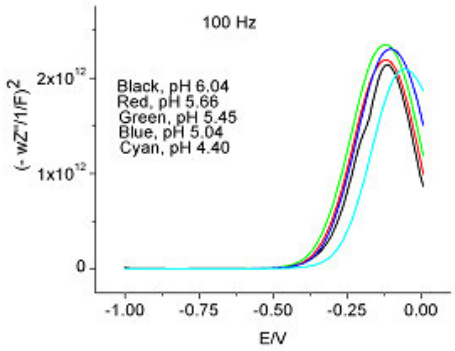

Figure 31. Mott-Schottky plot for 0.095 M sodium molybdate, pH 4.40 – 6.04, 100 Hz

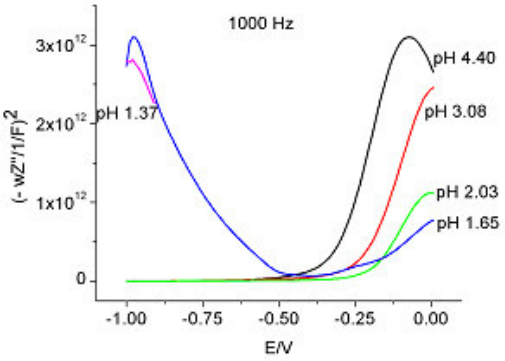

Figure 32. Mott-Schottky plot for 0.095 M sodium molybdate, below pH 4.40, 1000 Hz

Under our present experimental conditions, the behavior exhibited was not coming from the passivation of mercury. It might well be due to a molybdenum reduced species film formation and subsequent growth of this film, instead of the oxide film and oxide growth.

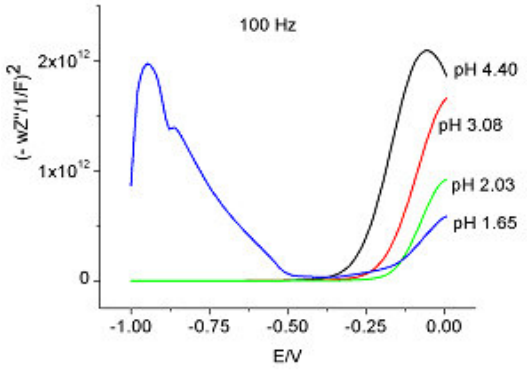

Figure 33. Mott-Schottky plot for 0.095 M sodium molybdate, below pH 4.40, 100 Hz

3.3. Nature of molybdenum species

It is well known that the simple molybdate, MoO_4^{2-}, condenses on acidification and the nature of the species formed depends heavily on the concentration of acid in solution. We have discussed the nature of the molybdenum (VI) species in aqueous solutions in some detail in the introduction.

In the past, metals and alloys were efficiently protected from corrosion in extreme conditions by chromates. However, chromates are now being replaced by other inhibitors, such as molybdates because of the extreme toxicity of chromates [29]. No serious attempt has been made to elucidate the influence of the nature of the aqueous molybdate present on the inhibition of corrosion by molybdate [29-35].

In the present study, we started with molybdenum(VI). It will be an equilibrium mixture of the simple molybdate or hepta-molybdate or octa-molybdate and their protonated species depending on the pH. One or more species should dominate, depending on the pH value.

The literature data on the reduction of molybdenum species are at high concentrations of acid [36-39]. We have studied the reduction of molybdenum (VI) under mild acid conditions because of the recent work on giant polyoxometalates [18].

The cyclic voltammetric data on the nature of aqueous molybdenum species are consistent with the potentiometric titration data.

The data in the literature on the nature of the molybdenum species adsorbed on the electrode have been inconclusive. It is agreed, however, that a reduced species is adsorbed. X-ray photoelectron spectra indicated molybdenum in both 4+ and 6+ oxidation states [34]. It has also been reported that with cathodic polarization, molybdates can be in the form of many states between Mo (III) and Mo (VI) [33]. It has also been suggested [29] that cathodic polarization at -2V (standard calomel electrode) produces the unstable compound $Mo(OH)_3/Mo_2O_3$. The $Mo(OH)_3$ formation at this potential has been attributed to the availability of OH^- ions formed on the electrode surface. The reaction is

$$MoO_4^{2-} + 8H^+ + 3e^- \rightarrow Mo^{3+} + 4H_2O$$

The $Mo(OH)_3$ compound is not stable and changes into more stable compounds by the successive reaction [29]

$Mo(OH)_3 + OH^- \rightarrow Mo(OH)_4$ (or $MoO_2.2H_2O$) $+ e^-$ or

$$Mo^{3+} + 2H_2O \rightarrow MoO_2 + 4H^+ + e^- \text{ or}$$

$$MoO_2^- \rightarrow MoO_2 + e^-$$

It is suggested that the following reaction can also proceed successively.

$$Mo^{3+} + 3H_2O \rightarrow MoO_3 + 6H^+ + 3e^-$$

$$E_o = 0.317 - 0.1182\ pH - 0.0197 \log(Mo^{3+}).$$

For an assumed concentration of 10^{-6} M for Mo^{3+}, E_o values of -0.99, -0.64, and -0.17V (standard calomel electrode) have been calculated [29]. The equilibrium and potential relationships between MoO_2 and MoO_3 are

$$MoO_2 + H_2O \rightarrow MoO_3 + 2H^+ + 2e^-$$

$$E_o = 0.320 - 0.0591\ pH$$

This gives E_o values of -0.52, -0.35, and -0.11V at pH 10, 7, and 3, respectively. Based on these assumptions, a duplex nature of MoO_2/MoO_3 film on aluminum was suggested. There is no reason why such a scenario cannot hold in our present studies using mercury.

It has been observed in XPS studies that as the potential is changed to less cathodic potentials, the signal intensity dominance changed from that Mo(IV) to that of Mo(VI). If this were true, during our admittance measurements when we scanned from negative to less negative potentials, the film thickness should increase and the ratio of the duplex species could also change. Thus the two peaks observed in admittance at pH 6.28 and the shift in peak potentials we observed at 100 Hz for the pH range 4-6 might also be due to the sensitivity of the duplex adsorbed species.

However we had attributed this behavior to the change in protonation of the species in solution. This question can be resolved only if we know the redox potentials of the different protonated species at any given pH.

The aqueous chemistry of Mo(V) in solutions with hydrogen ion concentration less than 2M suggests that the monomeric green form is unstable and easily changed into a stable, yellow orange or brown colored dimeric di-μ-oxo species, $Mo_2O_4^{2+}$, with two terminal oxo groups [40-43]. The structure suggested is

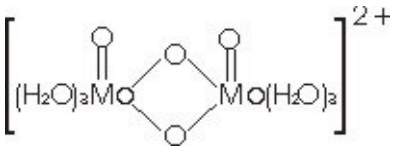

.

At acidities greater than 7M HCl, the green monomeric form is suggested [43].

Controversy also exists regarding the aqueous chemistry of Mo(IV) as to whether it is a monomer, MoO^{2+} or $Mo(OH)_2^{2+}$, or dimer, $Mo_2O_2^{4+}$ [44-46]. Monomeric Mo(IV) is viewed as a transient intermediate species during reduction of Mo(VI) or Mo(V) and that it would disproportionate to Mo(III) and Mo(V) [46]. The red colored dimeric form is given the formula

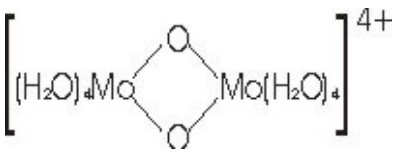

with a di-μ-oxo bridge similar to the dimeric Mo(V). The alternate structure with Mo-Mo bond and two terminal oxygen bonds is suggested as less probable [46].

The aqueous chemistry of Mo(III) suggests [47-49] a pale yellow monomeric $MoO(H_2O)_5^+$ or preferably $Mo(H_2O)_6^{3+}$ and a green di-μ-ol dimer, with a favored structure instead of $[(H_2O)_5Mo\text{-}O\text{-}Mo(H_2O)_5]^{4+}$.

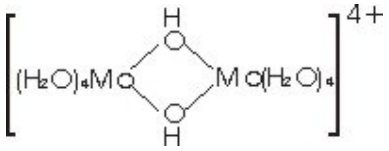

The complicated interrelationships between the chemistry of different species of Mo (III), Mo (IV), and Mo (V) are shown in the electrochemical studies [50] of molybdenum in oxidation states III-VI in noncomplexing trifluoromethane sulfonic acid , mostly at 2 M. It shows the color of Mo (III) species as pale yellow, yellow, blue-green and green, yellow Mo (V) and pink Mo (IV). The reduction is done at -0.75 V close to our cyclic voltammetric peaks.

3.4 Color Oscillations

We had observed during cyclic voltammetry, admittance and impedance measurements that the color of the mercury drop often changed depending on the pH, or potential or frequency. Sometimes the mercury drop retained the color of the adsorbed species even after allowing the drop to fall into the bulk solution. For example, the mercury drop retained the copper red color even after the cyclic voltammetry at pH 6-4. Below pH 4, the color of the final drop was dark blue. During admittance measurements at 1000 and 100 Hz or during impedance measurements at -0.8 or -0.6V, the color changed from brass to gold to copper red at pH 6.08. But there was no color oscillation. On the other hand at pH 5.64 to pH 2, the color changed at least 4 times in the beginning one minute from yellow to gold to copper to blue and finally stayed as dark blue on the mercury. The dropped mercury retained the dark blue color. At pH lower than 2, the aqueous solution became slightly blue. At pH 1.37, dark blue material was coming out of mercury into the bulk solution.

The same interference color phenomenon has been observed at different potentials and pH for electrode systems, such as aluminum, zinc, tinplate, stainless steel or platinum, in the presence of molybdates at different pH [29-30]. As far as we know, we have, for the first time, observed a frequency dependent color oscillation for molybdates.

While studying the effect of sodium molybdate on the pitting corrosion of aluminum, it was observed [29] that polarization at -2 V produced an unstable black sluggish layer on the electrode surface which changed into brown on exposure to open atmosphere for 3-4 hours. This could be easily wiped away. However on exposure to the atmosphere for 24 hours, a blackish dark brown film that could not be washed away, was formed. The unstable compound was attributed to $Mo(OH)_3/Mo_2O_3$ which was oxidized to $MoO(OH)_2.2H_2O/MoO_2$. The effect of sodium molybdate on the cathodic polarization of zinc [33] was to produce a “matt black” coating at pH 3 and 5, a blue sludge at pH 1 and a dark, “grey-fawn” coloration at pH 9 and 13. Cathodic polarization of tin plate in the presence of sodium molybdate [33] produced “faint gold and iridescent colors at pH 13 and 9, through a strong,

attractive iridescence at pH 5 to flaky black on mottled iridescence at pH 3". The iridescent film has been attributed to Mo (V), in the form of $MoO(OH)_3$ or $Mo_2O_3.3H_2O$. Cathodic polarization of platinum in the presence of sodium molybdate produced [33] "a lighter to medium gold coloration at pH 5 and a darker iridescent coating at pH 3". Other colors such as purple mauve, molybdenum blue, gold with pink red, goldgrey and dark gold were also observed depending on the pH and concentration of sodium molybdate. A sequence of colored films depending on the potential has also been observed [30] during the cathodic polarization of stainless steels and platinum in the presence of sodium molybdate and sodium chloride at different pH. At pH below 2, the observed blue film was attributed to molybdenum blue, a mixture of Mo (V) and Mo (VI) species. None of these authors discussed the role of the dimers of Mo (III), Mo (IV) and Mo (V) in the formation of these different films with a variety of colors.

4. CONCLUSIONS

The cyclic voltammetric data presented here suggest that the data can be roughly divided into 4 regions: pH 7-12 where only one species is active and exhibits no redox peaks; pH 6-7 where indications of protonated monomolybdates exist with characteristic redox peaks; pH 3-6 where molybdate condensation takes place with no sensitivity of redox for protonation of the hepta-molybdates; pH below 3 where further condensation seem to take place with shifts in redox potentials sensitive to the degree of protonation.

The impedance data are analyzed in terms of admittance, Nyquist and Bode plots, differential capacitance and Mott-Schottky plots after again dividing into different regions. Each region exhibits varying characteristics. Lower frequencies tend to discriminate among different protonated species or the different adsorbed species. Mott-Schottky plots reveal a change in semiconductor behavior of the adsorbed film from p-type at pH greater than 7, to n-type at pH 7-2, and a final duplex behavior below pH 2. Apart from the previous observations of potential and pH dependent color oscillations of the reduced molybdenum species, we have also observed a frequency-dependent color oscillation.

The impedance technique seems to be a powerful tool to provide a variety of information about the nature of isopolyoxomolybdates. More information is obtained about their characteristics than from potentiometry.

ACKNOWLEDGEMENTS

BC gratefully acknowledges the support of this work by the US Department of Energy (DEFG0286ER45237.023).

References

1. M.T. Pope, Chapter 3, p. 33 in "Heteropoly and Isopoly Oxometalates", Springer-Verlag, New York, 1983
2. C.L. Hill, Guest Editor, " Polyoxometalates" , Chem. Rev. January-February, Vol. 98, No.1, 1998
3. F. Taube, I. Andersson, and L. Pettersson, Chapter 11, p. 145 in "Polyoxometalate Chemistry From Topology via Self-Assembly to Applications", M.T. Pope and A. Muller Editors, Kluwer Academic Publishers, Boston, 2001

4. L. Pettersson, p. 139 in "Polyoxometalate Chemistry for Nano-Compsite Design", T. Yamase and M.T. Pope Editors, Kluwer Academic/Plenum Publishers, 2002
5. M.T. Pope, and A. Muller, *Angew Chem*., Intl. Ed. Engl., 30(1991) 34
6. C.L. Hill, C.M.P. McCartha, *Coord. Chem. Rev*., 143(1995) 407
7. Q. Chen, J.Zubieta, *Coord. Chem. Rev*., 114(1992) 107
8. T. Yamase, "Topics in Molecular Organization and Engineering 10: Polyoxometalates: From Platonic Solids to Antiretroviral Activity," ed. by M.T. Pope and A. Muller, Kluwer Academic Publishing, Netherlands, (1994) 241
9. Y. Sasaki and L.G. Sillen, *Acta Chem. Scand*., 18(1964) 1014
10. Y. Sasaki, I. Lindqvist, and L.G. Sillen, *J. Inorg. Nuclear Chem*., 9(1959) 93
11. G. Schwarzenbach, and J. Meier, *J. Inorg. Nuclear Chem*., 8(1958) 302
12. J.J. Cruywagen and J.B.B. Heyns, *Inorg. Chem*., 26(1987) 2569
13. J. Aveston, E.W. Anacker, and J.S. Johnson, *Inorg. Chem.,* 3(1964) 735
14. P.C.H Mitchell, *Quarterly Rev. of Chem. Society*, 20(1966) 103
15. M. Inoue, and T. Yamase, *Bull. Chem. Soc. Jpn*., 68(1995) 3055
16. R. Xi, B. Wang, K. Isobe, T. Nishioka, K. Toriumi, and Y. Ozawa, *Inorg. Chem*., 33(1994) 833
17. K.H. Tytko, B. Schonfeld, B. Buss, and O. Glemser, *Angew. Chem*. Int. Ed., 12(4)(1973) 330
18. A. Muller, E. Krickemeyer, H. Bogge, M. Schmidtmann, and F. Peters, *Angew. Chem*. Int. Ed., 37(1998) 3360
19. C.V. Krishnan, and M. Garnett, 226th ACS National Meeting, Abs. Inor. 0028, NY 2003
20. C.V. Krishnan, and M. Garnett, 204th Meeting of ECS, Abs. 1378, Orlando 2003
21. C.V. Krishnan, and M. Garnett, *Electrochimica Acta,* 51(2006) 1541
22. H.L. Friedman and C. V. Krishnan, in 'Thermodynamics of Ion Hydration' in "Water, A Comprehensive Treatise", Vol.3, Chapter 1, F. Franks editor, Plenum Press, (1973)
23. R.M. Diamond, *J.Phys. Chem*., 67(1963) 2513
24. F.A. Cotton, and G. Wilkinson, p. 938-940 in "Advanced Inorganic Chemistry, 2nd Revised and Augmented Edition, Interscience Publishers, John Wiley & Sons, New York 1966
25. V.D. Jovic, and B.M. Jovic, *J. Electroanal. Chem.,* 54(2003) 1
26. H. Tsuchiya, S. Fujimoto, and T. Shibata, *J. Electrochem. Soc.,* 151(2004) B39 and references therein
27. D.S. Kong, S.H.Chen, C. Wang, and W. Yang, *Corrosion Sci.*, 45(2003) 747 and references therein
28. N.E. Hakiki, M.D. Belo, A.M.P. Simoes, M.G.S. Ferreira, *J. Electrochem. Soc*., 145(1998) 3821
29. K.C. Emregul and A.A. Aksut, *Corrosion Sci.,* 45(2003) 2415
30. J.N. Wanklyn, *Corrosion Sci.,* 21(1981)211
31. C.B. Breslin, G. Treacy, and W.M. Carroll, *Corrosion Sci*., 36(1994) 1143
32. B.A. Shaw, G.D. Davis, T.L. Fritz, and K.A. Olver*, J. Electrochem. Soc*., 137(1990)359
33. G.D. Wilcox, D.R. Gabe, and M.E. Warwick, *Corrosion Sci.,* 28(1988) 577
34. A. Kh. Bairamow, S. Zakipour and C. Leygraf, *Corrosion Sci.,* 25(1985) 69
35. M.N. Hull, *J. Electroanal. Chem*., 38 (1972)143
36. M. Wolter, D.O. Wolf, and M.V. Stackelberg, *J. Electroanal. Chem*., 22(1969) 221
37. J.J. Wittick, and G.A. Rechnitz, *Anal. Chem.,* 37(1965) 816
38. I. M. Kolthoff and I. Hodara, *J. Electroanal. Chem*., 4(1962) 369
39. M.G. Johnson, and R.J. Robinson, *Anal. Chem.,* 24(1952) 366
40. M. Ardon and A. Pernick, *Inorg. Chem*., 12(1973) 2484
41. Y. Sasaki and A.G. Sykes, *J. Chem. Soc*., *Dalton Trans*., (1974)1968
42. J.T. Spence and M. Heydanek, *Inorg. Chem.,* 6(1967) 1489
43. L. Sacconi and R. Cini, *J. Am. Chem. Soc*., 76(1954) 4239

44. M. Ardon, A. Bino, and G. Yahav, *J. Am. Chem. Soc*., 98(1976) 2338
45. T. Ramasami, R.S. Taylor, and A.G. Sykes, *J. Am. Chem. Soc*., 97(1975) 5918
46. M. Ardon and A. Pernick, *J. Am. Chem. Soc*., 95(1973) 6871; 96 (1974) 1643
47. M. Ardon and A. Pernick, *Inorg. Chem*., 13(1974) 2275
48. A.R. Bowen, and H. Taube, *Inorg. Chem.,* 13(1974)2245
49. K. Kustin, and D. Toppen, *Inorg. Chem*., 11(1972) 2851
50. P. Chalilpoyil and F. C. Anson, *Inorg. Chem*., 17(1978)2418